

Shear wall thickness affects high-rise building internal force and horizontal displacement according to TCVN 2737:2023

Lam Thanh Quang Khai^{1*}, Ho Chi Cong²

¹ Faculty of Civil Engineering, Mien Tay Construction University, Vinh Long;

² Tuan Phong Consultancy Design and Construction Company Limited, Ben Tre.

KEYWORDS

shear wall,
stiffness,
building,
shear force,
displacement,
thickness,
axial force.

ABSTRACT

Shear walls increase the horizontal stiffness of multi-storey buildings in wind and earthquake conditions. According to TCVN 2737:2023, Etabs software must be used to study how shear wall thickness affects internal force and horizontal displacements in multi-storey buildings. This study examines the impact of varying initial shear wall thicknesses, starting with $b_w = 200\text{mm}$ and subsequently increasing to $b_w = 250\text{mm}$ (25%), $b_w = 300\text{mm}$ (50%), $b_w = 350\text{mm}$ (75%), and $b_w = 400\text{mm}$ (100%). The focus is on type I high-rise buildings (under 16-storey) and type II high-rise buildings (from 17 to 25-storey), specifically analyzing how these changes affect internal force and horizontal displacements at the building's top. The survey results of the 9-storey building indicate a 6% reduction in bending moment, a 13% increase in shear force, and a 7% increase in axial force when the shear wall thickness is increased by 100% compared to the original thickness. For the 21-storey building, increasing the shear wall thickness by 100% leads to a 31% reduction in the bending moment, a 47% reduction in the shear force, and a 12% reduction in the axial force compared to the original thickness. As the height of the building rises from 9 to 21-storey, the horizontal displacement increases by a ratio of 6.4 times in both directions.

1. Introduction

When exposed to horizontal loads, the frame and shear wall structural system experiences uneven deformation. This interaction serves as a key element of the system, enhancing the overall stiffness of the structure and minimising horizontal displacement [1]. The frame-shear wall structural system exhibits significant stiffness and a high capacity for bearing horizontal loads, making it a popular choice for medium- and high-rise buildings [2]. The initial examination of the frame-shear wall structure aids in comprehending the relationship between the frame and the shear wall, with calculations typically performed using analytical methods [3]. In this calculation, the shear wall is modelled as a cantilever bar experiencing bending deformation, while the frame is subjected to shear deformation. The connecting members are represented by rigid connecting beams, with the assumption of only horizontal force transmission [2], [4-5]. The perspective that a shear wall experiences bending without shear deformation could lead to imprecise results. The rotation of the connecting beams generates a bending moment that can alter the shear force distribution between the frame and the shear wall, highlighting the crucial role of the connecting beams in the interaction between these two structural elements [6-7].

An approximate method was developed to calculate the horizontal displacement for structures with non-uniform height and non-uniform stiffness, as proposed by Miranda and Reyes [8]. The

analytical transfer matrix method, utilised for shear wall frames with height-varying cross-sections and yielding precise results, was also suggested by Bozdogan [9] and Zhong et al. [10]. Research utilising the finite element method to provide approximate results was conducted by Bozdogan [11] and Son et al. [12]. Nevertheless, these studies overlooked the impact of the forced bending moment resulting from the connecting beams between the shear wall frames, as well as the shear deformation of the shear wall. The Badami and Suresh [13] utilised Etabs software to perform calculations using the finite element method, creating 3D models for various common structural systems. These included the reinforced concrete frame system, frame-shear wall system, rigid wall system with openings, and the outrigger structural system, all analysed under the influence of vertical loads and earthquakes.

Sangtiana et al. [14] conducted a study on a 53-storey building simulated by Etabs. The three structural models were positioned in four distinct earthquake zones. In addition to the mentioned study, Singh et al. [15] conducted an analysis of a 16-storey building utilising Etabs, aiming to identify the most appropriate structural system among those examined, thereby providing design engineers with a foundation for selecting the structural system for their projects. Sajjanshetty and Galanna [16] utilised Etabs software to examine a 24-storey building, aiming to compare the performance of various structural systems under vertical and horizontal loads.

Adnan et al. [17] conducted a study on the seismic resistance

*Corresponding author: Lamkhai@mtu.edu.vn

Received 04/10/2024, Revised 18/10/2024, Accepted 19/11/2024

Link DOI: <https://doi.org/10.54772/jomc.v14i02.798>

and structural damage of seismic moment frames. Nonlinear static analysis conducted with Sap2000 software demonstrated that the structure exhibits considerable seismic resistance, even under displacement conditions. In 2016, a shaking table test was carried out at the world's largest experimental facility, E-Defense, using a full-scale sample of a 6-story shear wall frame structure exposed to three-dimensional earthquake loads [18-19]. The research has offered valuable insights into the seismic resistance of structures and the advancement of experimental studies. Kim et al. [20] conducted an experimental study on a 6-story building featuring a shear wall frame structure to assess the seismic resistance of this structural system.

Alaghmandan et al. [21] conducted a structural study of 73 buildings. The research indicated that modifying the building's shape and creating a structural system capable of resisting lateral loads can mitigate the impact of wind loads. Sanada et al. [22] conducted a study to evaluate the seismic resistance of a rigid frame structural system using a designed scale model.

A shear wall is a structural element that significantly enhances the horizontal stiffness of multi-storey buildings when exposed to wind and earthquake forces, achieved through various arrangements of shear walls within the structure [23-30]. The behaviour of shear walls under horizontal loads varies with different load types and is influenced by several factors [31-34].

In the research conducted by Resmi and Roja [35], the authors showcased a range of studies examining the factors influencing the performance of shear walls. These studies, carried out by numerous scholars, aimed to analyse, evaluate, and provide insights on the location, shape, and various elements impacting the effectiveness of shear walls within the structural system. Wang et al. [36] proposed the application of the transfer matrix technique alongside structural modelling using wall elements to examine the response of shear wall frame structures under earthquake conditions. Coull and Puri [37] examined the impact of shear deformation in reinforced concrete double walls through an analysis method that employs a continuous connection technique. The authors discussed the predictions regarding deflection and stress for double walls that have cross-sections changing with height and are perforated with holes when exposed to horizontal loads. Shukla and Nallasivam [38] utilised Etabs software to model nine distinct cases of stiff wall configurations for a 30-storey building, aiming to explore the ideal placement of the stiff wall in response to vertical loads, wind loads, and seismic activity. More et al. [39] discuss the model of an 18-storey building featuring both symmetrical and asymmetrical plans. Shear walls were positioned at the corners and at the centre of the outer edge, while some areas were left without arrangement. Zahid et al. [30] conducted an analysis and evaluation of the shear wall arrangement's effectiveness for a 15-storey building under earthquake conditions, employing the equivalent static

method alongside Etabs software.

Three analytical models were developed using Etabs to examine the impact of shear wall placement in a 20-story building, carried out by the research team of Ahamad et al. [40]. Chandra et al. [41] conducted an experimental study on the interaction between shear and bending forces in shear walls, aiming to examine the nonlinear behaviour resulting from shear-bending under cyclic loading. Tianjian Ji et al. [42] examined the impact and significance of horizontal displacement based on load distribution and structural shape, highlighting the greater importance of the structure's shape factor.

Using numerical methods, [43-45] examined the impact of wind loads on columns and the geometric centre of both high-rise and low-rise buildings. The study focused on horizontal displacement at the top of buildings with frame and shear wall structures, according to TCVN 2737:2023. Research [46-47] examined the impact of basement stiff walls on the horizontal displacement at the top and the internal forces at the base of a column in a 16-story building featuring one basement, along with the effects of wind-related structural stiffness and stiffness reduction factors on the internal forces and horizontal displacement of the structure.

For almost three decades, Vietnam standard 2737:1995 [48] has played an important part in the basis of standards for the structural design of projects. Nonetheless, TCVN 2737:1995 presents certain issues, particularly regarding the calculation method for wind load. At present, TCVN 2737:2023 [49] has been released to solve the problems of TCVN 2737:1995 regarding the calculation method for wind load. Some studies on this issue have been calculating wind with aerodynamic coefficients derived from Appendix F.16 or surveying changes in reinforced concrete frame structures according to two standards TCVN 2737:1995 and TCVN 2737:2023 [50-51].

In this study, the authors examined how shear wall thickness affects internal force and horizontal displacement at the top of a multi-storey building. They utilised Etabs software for a consistent floor plan, comparing a 9-storey building (group I) with a 21-storey building (group II), according to the regulations set by The Council on Tall Buildings and Urban Habitat. The initial shear wall thickness of $b_w = 200\text{mm}$ was subsequently increased by 25% to $b_w = 250\text{mm}$, by 50% to $b_w = 300\text{mm}$, by 75% to $b_w = 350\text{mm}$, and finally by 100% to $b_w = 400\text{mm}$.

2. Materials and Methods

2.1. Model information of 9-storey and 21-storey buildings

Construction site: Vinh Long city, Vinh Long province, Vietnam

Project: Model 1 (M1) is a 9-storey building. Model 2 (M2) is a 21-storey building.

Basement and floor plans as Fig. 1 and Fig. 2

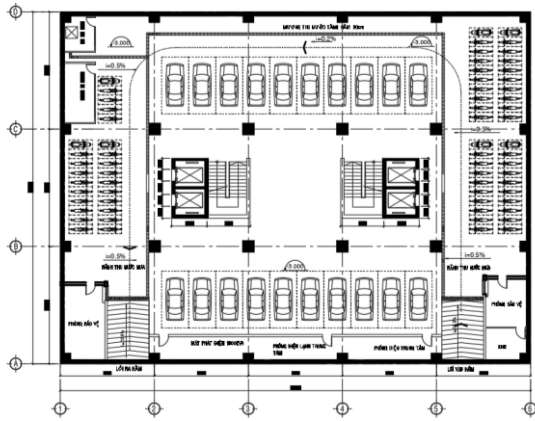


Fig. 1. Basement floor plan of M1 and M2.

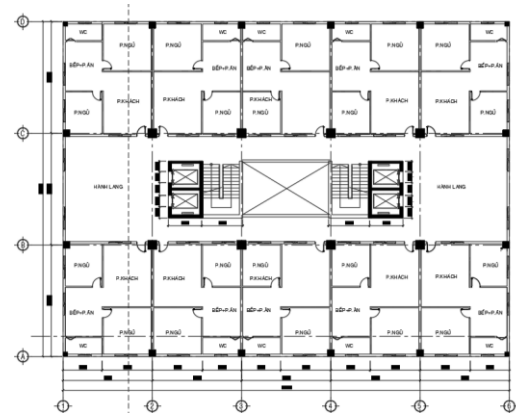


Fig. 2. Floor plans of M1 and M2.

The concrete (B25) and steel material (CB300-V) parameters. The initial shear wall thickness is $b_w = 200\text{mm}$, the floor thickness is 200mm for M1 and M2.

When arranging shear walls, the chosen shear wall cross-section corresponds to the column cross-section at the replacement location (refer to Table 1 and Table 2).

Table 1. Shear wall dimensions for M1.

	Storey	cross section 1 column	Shear wall = column		Column size
		$A_c \text{ (m}^2\text{)}$	$b_w \text{ (m)}$	$L_w \text{ (m)}$	(m)
W1-M1	Basement ÷ 3	0.49	0.2	2.45	0.7×0.7
W1-M1	Storey 4 ÷ 6	0.36	0.2	1.80	0.6×0.6
W1-M1	Storey 7 ÷ 9	0.25	0.2	1.25	0.5×0.5

Table 2. Shear wall dimensions for M2.

	Storey	cross section 1 column	Shear wall = column		Column size
		$A_c \text{ (m}^2\text{)}$	$b_w \text{ (m)}$	$L_w \text{ (m)}$	(m)
W2-M2	Basement ÷ 3	1.21	0.2	6.05	1.1×1.1
W2-M2	storey 4 ÷ 6	1.00	0.2	5.00	1.0×1.0
W2-M2	storey 7 ÷ 9	0.81	0.2	4.05	0.9×0.9
W2-M2	storey 10 ÷ 12	0.64	0.2	3.20	0.8×0.8
W2-M2	storey 13 ÷ 15	0.49	0.2	2.45	0.7×0.7
W2-M2	storey 16 ÷ 18	0.36	0.2	1.80	0.6×0.6
W2-M3	storey 19 ÷ 21	0.25	0.2	1.25	0.5×0.5

Wind load is determined according to TCVN 2737:2023, including two components W_x and W_y (not considering the torsional component). W_k is determined as the building located in Vinh Long City, models M1 and M2 are both in terrain type B, wind pressure belongs to zone II, see table 5.1 QCVN 02:2022/BXD [52].

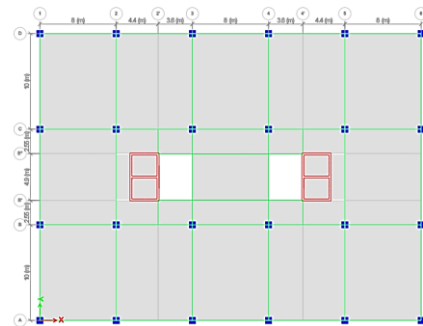
2.2. Construction site plan:

Model 1 (M1): 9-storey building, frame system (including columns, beams, floors) and shear wall at the elevator location as shown in Fig. 3.

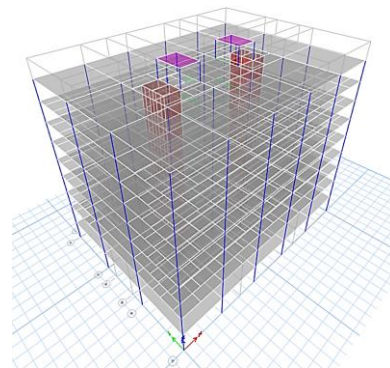
The wind loads in X and Y directions in Etabs in M1, are shown in Fig. 4.

Model 2 (M2): 21-storey building, frame system (including columns, beams, floors) and shear wall at the elevator location as shown in Fig. 5.

The wind loads in X and Y directions in Etabs in M2 model, are shown in Fig. 6.



a) M1 model floor plan



b) 3D model of M1

Fig. 3. M1 model.

Number of Load Sets

1

☒ Loads are Reversible for Combos

Load Set 1 of 1

Story	Diaphragm	Fx kN	Fy kN	Mz kN-m	X Ordinate m	Y Ordinate m
Story9	D1	111,6	0	0	20	15
Story8	D1	119,3	0	0	20	15
Story7	D1	119,3	0	0	20	15
Story6	D1	119,3	0	0	20	15
Story5	D1	119,3	0	0	20	15
Story4	D1	119,3	0	0	20	15
Story3	D1	119,3	0	0	20	15
Story2	D1	131,2	0	0	20	15
Story1	D1	114,2	0	0	20	15

a) wind load in X direction

Number of Load Sets

1

☒ Loads are Reversible for Combos

Load Set 1 of 1

Story	Diaphragm	Fx kN	Fy kN	Mz kN-m	X Ordinate m	Y Ordinate m
Story9	D1	0	154,2	0	20	15
Story8	D1	0	166	0	20	15
Story7	D1	0	166	0	20	15
Story6	D1	0	166	0	20	15
Story5	D1	0	166	0	20	15
Story4	D1	0	166	0	20	15
Story3	D1	0	166	0	20	15
Story2	D1	0	182,6	0	20	15
Story1	D1	0	158,9	0	20	15

b) wind load in Y direction

Fig. 4. The wind loads in X and Y directions in Etabs in M1.

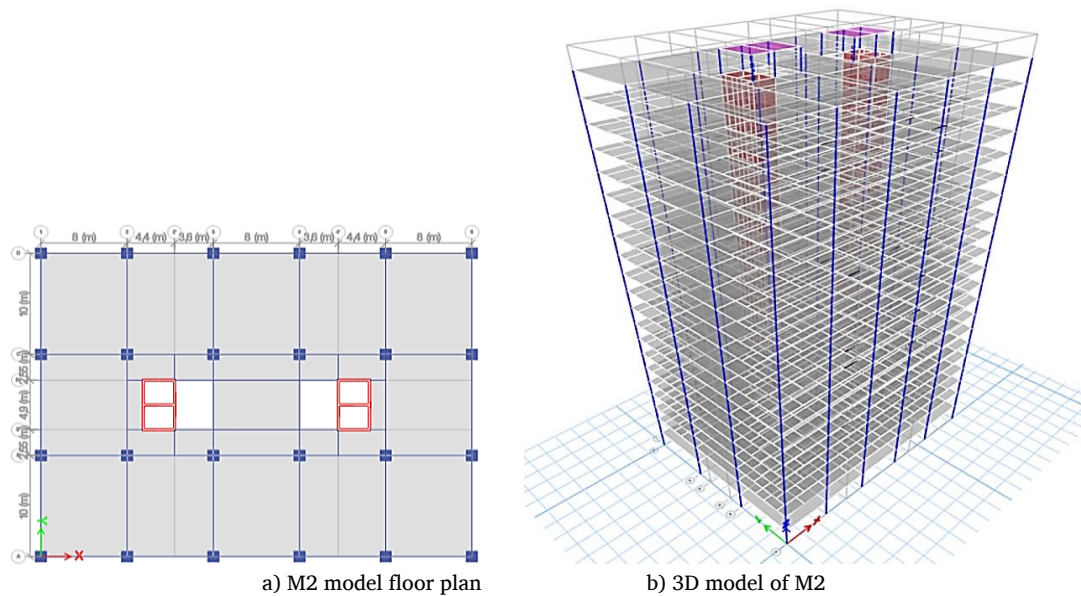


Fig. 5. M2 model.

Story	Diaphragm	Fx kN	Fy kN	Mz kN-m	X Ordinate m	Y Ordinate m
Story21	D1	159,3	0	0	20	15
Story20	D1	171,6	0	0	20	15
Story19	D1	171,6	0	0	20	15
Story18	D1	171,6	0	0	20	15
Story17	D1	171,6	0	0	20	15
Story16	D1	171,6	0	0	20	15
Story15	D1	171,6	0	0	20	15
Story14	D1	171,6	0	0	20	15
Story13	D1	171,6	0	0	20	15
Story12	D1	152,4	0	0	20	15
Story11	D1	150,1	0	0	20	15
Story10	D1	146,7	0	0	20	15
Story9	D1	143,4	0	0	20	15
Story8	D1	142,2	0	0	20	15
Story7	D1	142,2	0	0	20	15
Story6	D1	142,2	0	0	20	15
Story5	D1	142,2	0	0	20	15
Story4	D1	142,2	0	0	20	15
Story3	D1	142,2	0	0	20	15
Story2	D1	156,5	0	0	20	15
Story1	D1	136,1	0	0	20	15

a) wind load in X direction

Story	Diaphragm	Fx kN	Fy kN	Mz kN-m	X Ordinate m	Y Ordinate m
Story21	D1	0	206,6	0	20	15
Story20	D1	0	222,5	0	20	15
Story19	D1	0	222,5	0	20	15
Story18	D1	0	222,5	0	20	15
Story17	D1	0	222,5	0	20	15
Story16	D1	0	222,5	0	20	15
Story15	D1	0	222,5	0	20	15
Story14	D1	0	222,5	0	20	15
Story13	D1	0	222,5	0	20	15
Story12	D1	0	222,5	0	20	15
Story11	D1	0	196,1	0	20	15
Story10	D1	0	196,1	0	20	15
Story9	D1	0	196,1	0	20	15
Story8	D1	0	196,1	0	20	15
Story7	D1	0	196,1	0	20	15
Story6	D1	0	196,1	0	20	15
Story5	D1	0	196,1	0	20	15
Story4	D1	0	196,1	0	20	15
Story3	D1	0	196,1	0	20	15
Story2	D1	0	215,7	0	20	15
Story1	D1	0	187,7	0	20	15

b) wind load in Y direction

Fig. 6. The wind loads in X and Y directions in Etabs in M2 model.

3. Results and discussions

3.1. M1 model: Results of internal force and horizontal displacement

The results of internal force at the column base (axis 2/B) and

horizontal displacement at the top of M1 when increasing the thickness of b_w , shown in Table 3 and Table 4.

Table 3. Comparison of internal force at the column base (axis 2/B) of M1.

b_w (mm)	200	250	300	350	400
M3-3_kNm (bending moment)	134.98	130.28	127.91	127.09	127.36
V2-2_kN (shear force)	59.98	61.12	62.97	65.30	67.96
P_kN (axial force)	10,907.64	11,093.88	11,278.87	11,463.46	11,648.12
% difference M3-3		-3%	-5%	-6%	-6%
% difference V2-2		2%	5%	9%	13%
% difference P		1.71%	3.40%	5.10%	6.79%

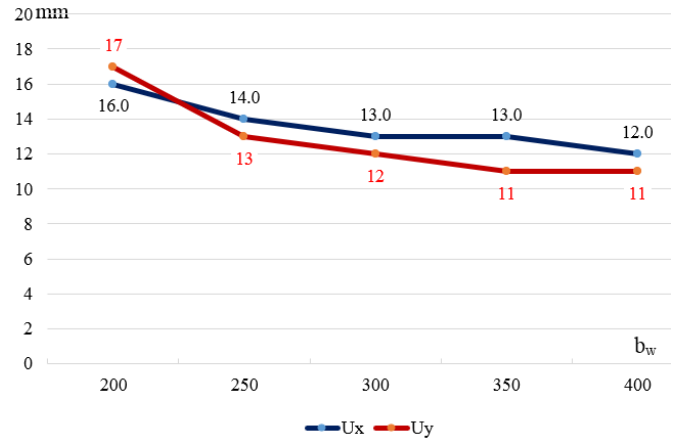
Table 4. Comparison of horizontal displacement at the top of M1

b_w (mm)	200	250	300	350	400
U_x (mm)	16	14	13	13	12
U_y (mm)	17	13	12	11	11
% difference U_x		-13%	-19%	-19%	-25%
% difference U_y		-24%	-29%	-35%	-35%

The horizontal displacement diagram at the top when changing b_w of M1 is shown in Fig. 7.

In Fig. 7, as the shear wall thickness rises from 25% to 100% of the initial thickness (with each increase being 25%), the horizontal displacement in the x direction decreases in proportion to each increment in shear wall thickness. However, an exception occurs when the thickness is increased from 50% to 75% (from $b_w=300\text{mm}$ to

$b_w=400\text{mm}$), where the horizontal displacement at the top remains unchanged. In a similar manner, the horizontal displacement in the y direction decreases proportionally with each increase in shear wall thickness. However, when the wall thickness is increased from 75% to 100% (from $b_w=350\text{mm}$ to $b_w=400\text{mm}$), there is no change in the horizontal displacement at the top. Figure 7 shows that the horizontal displacement at the top of the M1 model in the y direction decreases more significantly than the horizontal displacement at the top of the structure in the x direction, due to the greater length in the x direction compared to the y direction.

**Fig. 7.** The horizontal displacement diagram at the top when changing b_w of M1 (mm).

The internal force of the column base (axis 2/B) during the change of b_w in M1 is shown in Fig. 8.

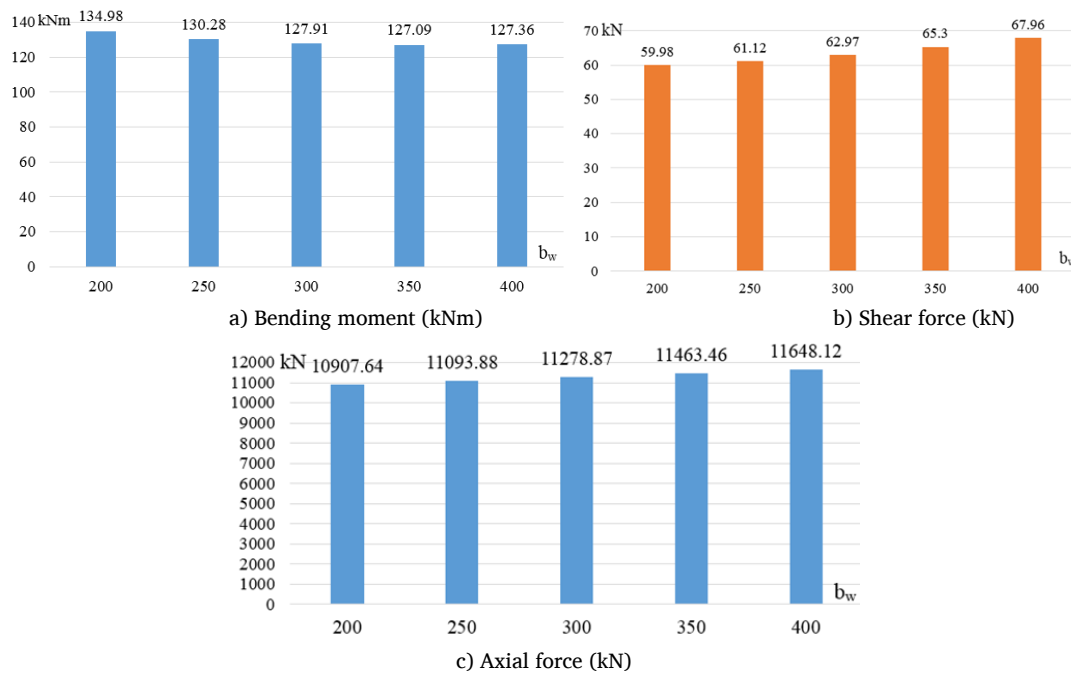
**Fig. 8.** Internal force diagram of column base (axis 2/B) when changing b_w of M1.

Fig. 8 shows that as the shear wall thickness increases, the internal force at the column base (axis 2/B) experiences a minimal reduction in bending moment, with the maximum decrease being only 6% when the shear wall thickness reaches 75% and 100% in comparison to the initial thickness. Unlike the bending moment, an increase in shear wall thickness leads to a gradual rise in both shear force and axial force corresponding to each load level of the shear wall thickness. As the thickness of the shear wall rises from 25% to 100% of its initial thickness, the shear force experiences an increase from 2% to 13% relative to its initial value. As the thickness of the shear wall increases from 25% to 100% of the initial thickness, the axial force rises from 1.71% to 6.79% relative to the initial axial force value.

3.2. M2 model: Results of internal force and horizontal displacement

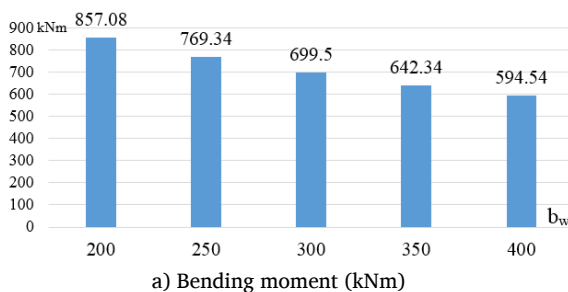
The results of the internal force at the column base (axis 2/B) are presented in Table 5, while the horizontal displacement at the top of M2 is detailed in Table 6, reflecting the changes when the shear wall thickness is increased from the initial value of $b_w = 200\text{mm}$ (negative values in the table indicate decreases from the initial value, whereas positive values indicate increases).

Table 5. Comparison of internal force at the column base (axis 2/B) of M2.

b_w (mm)	200	250	300	350	400
M3-3_kNm (bending moment)	857.08	769.34	699.50	642.34	594.54
V2-2_kN (shear force)	103.89	87.50	74.41	63.70	54.76
P_kN (axial force)	18,379.08	17,682.40	17,112.83	16,636.36	16,230.28
% difference M3-3		-10%	-18%	-25%	-31%
% difference V2-2		-16%	-28%	-39%	-47%
% difference P		-3,79%	-6,89%	-9,48%	-11,69%

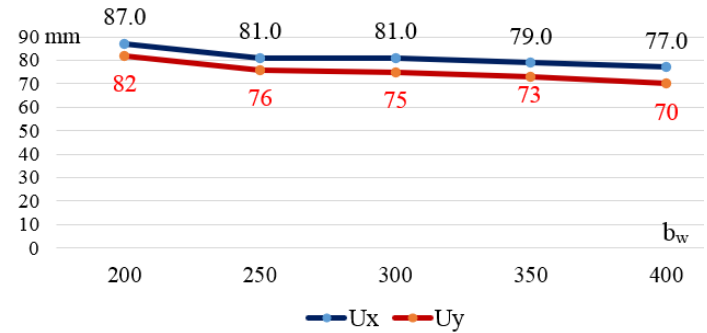
Table 6. Comparison of horizontal displacement at the top of M2.

b_w (mm)	200	250	300	350	400
U_x (mm)	87	81	81	79	77
U_y (mm)	82	76	75	73	70
% difference U_x		-7%	-7%	-9%	-11%
% difference U_y		-7%	-9%	-11%	-15%



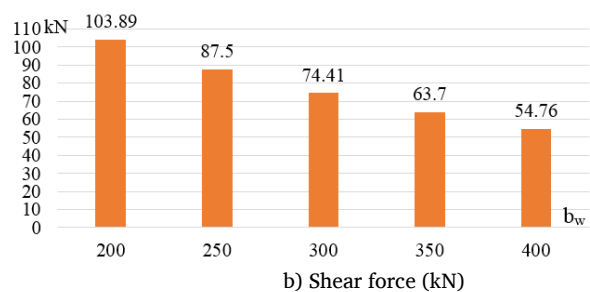
The horizontal displacement diagram of M2 is shown in Fig. 9

In Fig. 9, as the thickness of the shear wall increases relative to the initial thickness, there is a proportional decrease in horizontal displacement in both the x and y directions. In the x direction, the horizontal displacement at the top reduces by 7% with a 25% increase in shear wall thickness and by 11% with a 100% increase compared to the initial thickness. In the y direction, the horizontal displacement at the top reduces by a minimal 7% when the shear wall thickness is increased by 25%, and by 15% when the thickness is increased by 100% in comparison to the initial value. This indicates that the displacement in the y direction diminishes more significantly than the displacement in the x direction.



The internal force of the column base (axis 2/B) of M2 is shown in Fig. 10.

Figure 10 shows that as the thickness of the shear wall increases, there is a corresponding decrease in the internal force of the column base with each increment. Nonetheless, there is a notable reduction in the bending moment and shear force, whereas the axial force remains relatively unchanged. The bending moment reduces from 10% to 31% as the shear wall thickness increases from 25% to 100% in relation to the initial value. The shear force ratio ranges from 16% to 47%, while the axial force ratio varies from 3.79% to 11.69% in relation to the initial value. The thickness of the shear wall significantly influences the bending moment and shear force at the column base, whereas the axial force has an impact, though to a lesser extent.



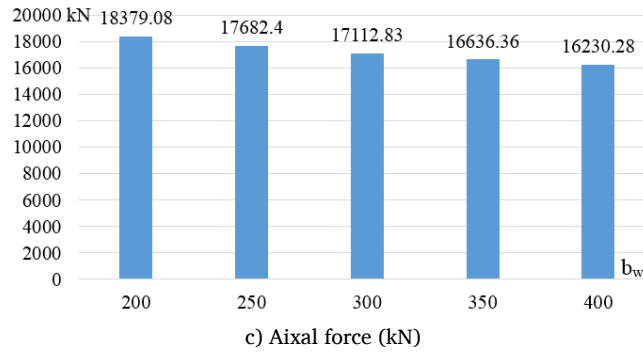


Fig. 10. Internal force diagram of column base (axis 2/B) when changing b_w of M2.

3.3. Comparison between M1 and M2

Assessing the internal force of the column base (axis 2/B) to compare and evaluate survey results between model M1 (9-storey) and model M2 (21-storey). The results of the comparison are presented in Fig. 11.

Fig. 11 shows that as the shear wall thickness rises from 25% to 100% of the initial value (with each increment being 25%), the bending moment at the column base of model M1 (9-storey) and M2 (21-storey) consistently diminishes with each increase. In model M2, the shear force and axial force of the column base show a gradual decrease, similar to the bending moment. Conversely, in model M1, both the shear force and axial force of the column base rise with each increment in shear wall thickness. As the thickness of the shear wall

risks to 75% of the initial value, the shear force in model M1 surpasses that of model M2 by an amount of 2.5%. This resembles the scenario where the shear wall thickness doubles to 100% of the initial value, yet the increase ratio is now 24.1%.

The horizontal displacement at the top of model M1 and M2 with increasing b_w is shown in Fig. 12.

Fig. 12 shows that when the shear wall thickness is increased to 100% of the initial value, the horizontal displacement at the top in the x direction of model M1 (is 6.4 times smaller than that of model M2. This ratio is 5.4 times when the shear wall thickness reaches 25% of the initial value. In the y direction, similar to the x direction, when the shear wall thickness reaches 25% of the initial value, the horizontal displacement of M1 is 4.8 times less than that of M2.

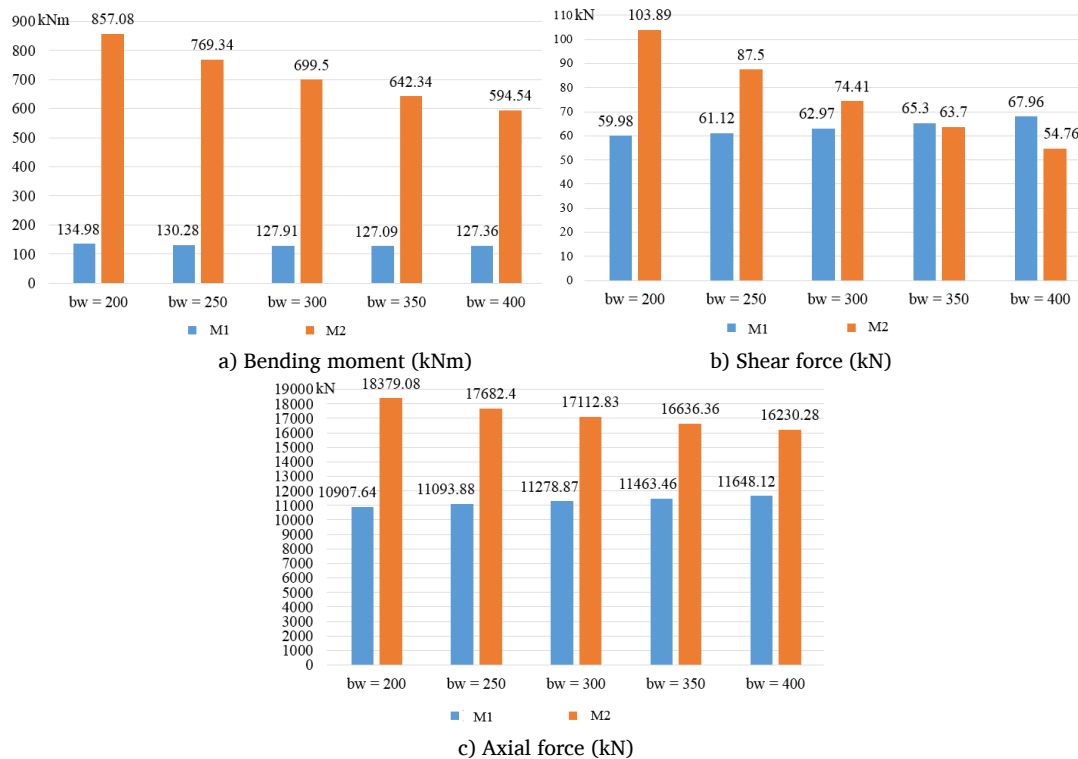


Fig. 11. Internal force of column base (axis 2/B) of M1 and M2 models.

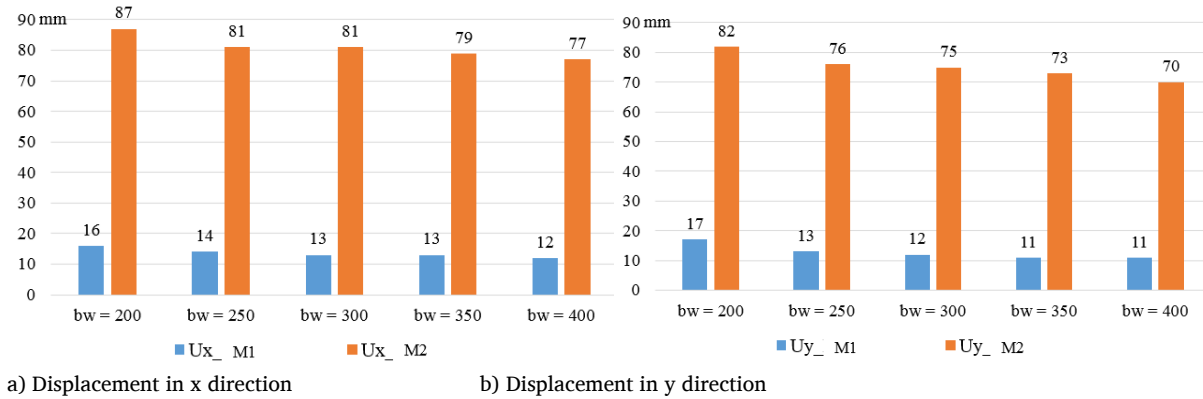


Fig. 12. Horizontal displacement at the top of M1 and M2 models (mm).

3.4. Assess and analyse the results of this study in relation to existing research:

The study used Etabs software to analyse a 24×32 m building which includes 22-storey and one basement. Loads and impacts were determined according with TCVN 2737:2023. The internal force results of the reinforced concrete column base, as compared between [44] and this study, are presented in Table 7.

Table 7. Comparison of internal force results.

	Research [44]	This study	% difference
Shear force V2-2 (kN)	259.4	294.99	13.7%
Axial force P (kN)	18187	21483	18.1%

The variations in the number of storey, member sizes, beam spans, and column spacing will result in differences in the internal force at the column base based on the calculated loads. Nonetheless, this variation is suitable, particularly concerning the shear force and axial force (not surpassing 20%). Thus, it can be concluded that the research data is both appropriate and reliable.

4. Conclusions

The following are some of the conclusions that may be derived from the results of the study:

1. The coefficient $k(z_e)$ is established via the equivalent height z_e , which is influenced by the building's height (h) and the width of the building that is perpendicular to the wind direction (b). Consequently, accurately determining the correct equivalent height z_e plays an important role in the calculation. In a 20-storey building, when h exceeds $2b$ in the section $z_e = z$, $k(z_e)$ shows a gradual increase.

2. The coefficient c for the various types of structures outlined in Appendix F is contingent upon the ratio h/d . This coefficient is segmented into regions that must be meticulously defined throughout

the calculation process.

3. The internal force at the column base of a 9-storey building indicates that increasing the shear wall thickness does not lead to a substantial reduction in the bending moment, with only a 6% decrease observed when the shear wall thickness reaches 100% of the initial value. Conversely, augmenting the thickness of the shear wall leads to a rise in both shear force and axial force with each increment (shear force rises by 13% and axial force by 7% when the shear wall thickness reaches 100% of its initial value).

4. The internal force of the 21-storey building shows that as the shear wall thickness increases, there is a gradual decrease in the bending moment, shear force, and axial force at the column base. Specifically, the bending moment decreases by 31%, the shear force decreases by 47%, and the axial force decreases by 12% when the wall thickness reaches 100% of the initial value.

5. Increasing the shear wall thickness for high-rise buildings will progressively decrease the internal force of the column base with each increment in shear wall thickness. In low-rise buildings, the bending moment at the column base is minimally reduced, while the shear force and vertical force at the column base increase with each increment in shear wall thickness.

6. Horizontal displacement: as the thickness of the shear wall increases, the horizontal displacement at the top in the y direction decreases more significantly than in the x direction (due to the greater length of the x direction compared to the y direction). Increasing the shear wall thickness is more effective in reducing the horizontal displacement at the top for low-rise buildings compared to high-rise buildings. As the height of the building rises from 9-storey to 21-storey, the horizontal displacement at the top escalates by a factor of 6.4 in both directions.

References

- [1]. N.T. Chuong, *Structural analysis of multi-storey buildings*. Hanoi: Construction Publishing House, 2018.

- [2]. S.B. Smith and A. Coull, *Tall Building structures: Analysis and Design*, Willy and Son, New York, 1991.
- [3]. D. Capuani, M. Merli and M. Savoia, *Dynamic analysis of coupled shear wall-frame systems*, Journal of sound and Vibration, 192(4), 867-883, 1996. DOI: 10.1006/jsvi.1996.0222
- [4]. Y.K. Park, H.S. Kim and D.G. Lee, *Efficient structural analysis of wall-frame structures*, The structural design of tall and special buildings. 23(10), 740-759, 2014. DOI: 10.1002/tal.1078
- [5]. I. Kazaz and P. Gülkan, *An alternative frame-shear wall model: continuum formulation*, The structural design of tall and special buildings. 21(7), 524-542, 2012. DOI: 10.1002/tal.626
- [6]. A. Surahman, *Modeling effects on forces in shear wall-frame structures*, Journal of Engineering and Technological sciences, 47(2), 117-125, 2015. DOI: 10.5614/j.eng.technol.sci.2015.47.2.1
- [7]. X. Guiyun, W. Shu and I. Stanculescu, *Efficient analysis of shear wall-frame structural systems*, Engineering Computation, 2019. DOI: 10.1108/EC-12-2018-0568
- [8]. E. Miranda and C.J. Reyes, *Approximate lateral drift demands in multistory buildings with nonuniform stiffness*, Journal of structural Engineering, 128(7), 840-849, 2002. DOI: 10.1061/(ASCE)0733-9445(2002)128:7(840)
- [9]. K.B. Bozdogan, *A approximate method for static and dynamic analyses of symmertric wall-frame buildings*, The structural design of tall and special buildings, 18(3), 279-290, 2009. DOI: 10.1002/tal.409
- [10]. H. Zhong, Z. Liu, H. Quin and Y. Liu, *Static analysis of thin-walled space frame structures with arbitrary closed cross-sections using transfer matrix method*, Thin-Walled structures, 123, 255-269, 2018. DOI: 10.1016/j.tws.2017.11.018
- [11]. K.B. Bozdogan, *A method for lateral static and dynamic analyses of wall-frame buildings using one dimensional finite element*, Scientific Research and Essays, 6(3), 616-626, 2011. DOI: 10.5897/SRE10.863
- [12]. H.J. Son, J. Park, H. Kim, Y. H. Lee and D.J. Kim, *Generalized finite element analysis of high-rise wall-frame structural systems*, Engineering computations, 34(1), 189-210, 2017. DOI: 10.1108/EC-07-2016-0266
- [13]. S. Badami and M.R. Suresh, *A study on behavior of structural systems for tall buildings subjected to lateral loads*, International Journal of engineering research & Technology, 3(7), 989-994, 2014.
- [14]. S. Sangtiani, J. Simon, J. Satyanarayana and D. Sangtiani, *Performance of tall buildings under lateral loads with different type of structural system*, International Journal of Civil Engineering and Technology (IJCIET), 8(3), 1014-1022, 2017.
- [15]. H. Singh, A.K. Tiwary, S. Thakur and G. Thakur, *Performance evaluation of high-rise reinforced concrete buildings under dynamic loading considering different structural systems*, Material today: Proceeding, 2023. DOI: 10.1016/j.matpr.2023.08.251
- [16]. M.B. Sajaanshetty and P.Galanna, *A study on static and dynamic behaviour of Outrigger structural system for different structural configuration*, Journal of scientific research and technology, 1(7), 37-52, 2023. DOI: 10.5281/zenodo.10045307
- [17]. A.B. Adnan, M.H. Osman, I. Faridmehr and R. Hodzati, *Sesmic Assessment of RC building according to FEMA 356*, International Journal of Earth sciences and engineering, 6(7), 1488-1496, 2013.
- [18]. T. Kabeyasawa, T. Matsumori, H. Katsumata and K. Shirai, *Design of the full-scale six-story reinforced concrete wall-frame building for testing at E-Defense*, Proceedings of the first NEES/E-Defense workshop on collapse simulation of reinforced concrete building structures, Berkeley, US, 23-46, 2005.
- [19]. K. Shirai, T. Matsumori and T. Kabeyasawa, *Simulated Earthquake test on a full-scale six-story reinforced concrete building at E-Defense, Part 2: Study on distribution of seismic force*, Proceedings of the second NEES/E-Defense workshop on collapse simulation of reinforced concrete building structures, Miki Japan, 17-28, 2006.
- [20]. Y. Kim, T. Kabeyasawa, T. Matsumori and T. Kabeyasawa, *Numerical study of a full-scale six-story reinforced concrete wall-frame structure tested at E-Defense*, Earthquake engineering & structural dynamic, 41(8), 1217-1239, 2012. DOI: 10.1002/eqe.1179
- [21]. M. Alaghmandan, B. Bahrami and M. Elnimeiri, *The future trend of architectural form and structural system in High-Rise Buildings*, Architectural Research, 4(3), 55-62, 2014. DOI: 10.5923/j.arch.20140403.01
- [22]. Y. Sanada, T. Kabeyasawa and Y. Nakano, *Analyses of reinforced concrete wall-frame structural systems considering shear softening of shear wall*, In Proc., 13th world conference on Earthquake Engineering, Canada, paper No. 3036, 2004.
- [23]. A. Tena-Colunga and M. A. Pérez-Osornio, *Impact of shear deformations on the location of the centers of torsion of shear wall buildings*, Proceedings, Seventh US National Conference on Earthquake Engineering (7NCEE), Massachusetts, 193, 2002.
- [24]. A. Tena-Colunga and M. A. Pérez-Osornio, *Assessment of shear deformations on the seismic response of asymmetric shear wall buildings*, Journal of Structural Engineering, 131(11), 1774-1779, 2005. DOI: 10.1061/(ASCE)0733-9445(2005)131:11(1774)
- [25]. T.J. Sullivan, M.J.N. Priestley, G.M. Calvi, *Direct displacement-based design of frame-wall structures*, Journal of Earthquake Engineering, 10(sup001), 91-124. DOI: 10.1080/13632460609350630
- [26]. B.T. Lam, *Research on influences of shear walls location to torsion and displacement of high-rise buildings under transverse loading*, The University of Danang - Journal of Science and Technology, 2(25), 2008.
- [27]. H.H.A. Abd-el-Rahim and A.A.E.R. Faraghy, *Role of shear walls in high rise buildings*, Journal of Engineering Sciences, 38(2), 403-420, 2010. DOI: 10.21608/jesaun.2010.124373
- [28]. A.S. Agrawal and S.D. Charkha, *Effect of change in shear wall location on storey drift of multistorey building subjected to lateral loads*, International Journal of Engineering Research and Applications, 2(3), 1786-1793, 2012.
- [29]. P.S. Kumbhare and A.C. Saoji, *Effectiveness of Changing Reinforced Concrete Shear Wall Location on Multi-storeyed Building*, International Journal of Engineering Research and Applications, 2(5), 1072-1076, 2012.
- [30]. C.Z.B. Zahid, S. Alam, A. Fahik, M.I. Khan and T.U. Mohammed, *Different orientations of shear wall in a reinforced concrete structure to control drift and deflection*, Journal of Physics: Conference Series, 2521, 012006, 2023. DOI: 10.1088/1742-6596/2521/1/012006
- [31]. K. Orakcal, L.M. Massone and J.W. Wallace, *Analytical modeling of reinforced concrete walls for predicting flexural and coupled-shear-flexural responses*, PEER Report 2006/07, Pacific Earthquake Engineering Research Center, University of California, Los Angeles, October 2006.
- [32]. T. Eimani, *Analytical modeling of reinforced concrete shear wall structures*, PhD dissertation, University of Southern California, Los Angeles, California, May 1997.
- [33]. T. Paulay and M.J.N. Priestley, *Seismic Design of Reinforced Concrete and Masonry Buildings*, A Wiley Interscience Publication John Wiley and Sons, Inc, 1992.
- [34]. V.V. Bertero, *Seismic behaviors of RC wall structure system*, In 7th World conference on Earthquake Engineering, Istanbul, Turkey, September 1980, volume 6, pages 323-330.

- [35]. R. Resmi and S. Roja, *A review on performance of shear wall*, International Journal of applied engineering research, 11(3), 369-373 2016.
- [36]. Q. Wang, L. Wang and Q. Liu, *Effect of shear wall height on earthquake response*, Engineering structures, 23, 376-384, 2001. DOI: 10.1016/S0141-0296(00)00044-4
- [37]. A. Coull and R.D. Puri, *Analysis of coupled shear walls of variable cross-section*, Building Sciences, 2(4), 313-320, 1968. DOI: 10.1016/0007-3628(68)90011-X
- [38]. K. Shukla and K. Nallasivam, *Effective location of shear walls in High-Rise RCC buildings subjected to lateral loads*, Civil Engineering Infrastructures Journal, 57(1), 103-117, 2024. DOI: 10.22059/CEIJ.2023.350020.1879
- [39]. M.R. More, A.S. Bhumare and S.B. Nagargoje, *The impact of different shear wall structure position on symmetric and Unsymmetric tall buildings*, International Journal for research in applied Science & Engineering technology, 11(4), 2023. DOI: 10.22214/ijraset.2023.50308
- [40]. S.A. Ahamad and K.V. Pratap, *Dynamic analysis of G+20 multi storied building by using shear walls in various locations for different seismic zones by using Etabs*, Materials today: Proceedings, 43, 1043-1048, 2021. DOI: 10.1016/j.matpr.2020.08.014
- [41]. J. Chandra, G. Milla and J.A. Tambuna, *Evaluation of shear-flexure interaction behavior of reinforced concrete wall*, Civil Engineering Demesion, 2024, 26(1), 11–20. DOI: 10.9744/ced.26.1.11-20
- [42]. T. Ji, B.R. Ellis and A.J. Bell, *Horizontal movements of frame structures induced by vertical loads*, Proceedings of the Institution of Civil Engineers – Structures and Buildings, 156(2), 141-150, 2003. DOI: 10.1680/stbu.2003.156.2.141
- [43]. Lam, T.Q.K. *Impact of wind loads on columns or the building's geometric center in high-rise and low-rise buildings*. Multidisciplinary Science Journal, 6(6), 2024091, 2023. DOI: 10.31893/multiscience.2024091
- [44]. Lam, T. Q. K. *Horizontal displacement at the top of the building with frame and shear walls structures according to TCVN 2737:2023*. Multidisciplinary Science Journal, 6(7), 2024121, 2024. DOI: 10.31893/multiscience.2024121
- [45]. Lam, T. Q. K. *The influence of the layout of shear walls on internal forces and horizontal displacements in an 18-story building*. Edelweiss Applied Science and Technology, 8(3), 259–278. 2024. DOI: 10.55214/25768484.v8i3.963
- [46]. Do, T.M.D. *Horizontal displacement of high-rise buildings with and without basement shear walls*. Multidisciplinary Science Journal, 6(6), 2023 2024093. DOI: 10.31893/multiscience.2024093
- [47]. Do, T. M. D. *Wind-related structural stiffness and stiffness reduction factors*. Multidisciplinary Science Journal, 6(9), 2024, 2024181. DOI: 10.31893/multiscience.2024181
- [48]. TCVN 2737:1995, *Loads and Actions norm for design*, Vietnam Standard, 1995.
- [49]. TCVN 2737:2023, *Loads and actions*, Vietnam Standard, 2023.
- [50]. T.S.S. Hoach, *Calculation of wind load for building with square and rectangular plans according to TCVN 2737:2023*. Journal of Science, Technology and Engineering Mien Tay Construction University, 7, 8-17, 2023.
- [51]. T.V. Tam, *Investigation of changes in design of frame structures and pile foundation of reinforced concrete buildings according to two design standards TCVN 2737-1995 and TCVN 2737-2023*, Journal of Construction, 3, 82-87, 2024.
- [52]. [QCVN 02:2022/BXD, *National Technical Regulation on Natural Physical and Climatic Data for Construction*, 2002.